

Correlation between electrical transport, microstructure and room temperature ferromagnetism in 200 keV Ni²⁺ ion implanted zinc oxide (ZnO) thin films

B. Joshi · S. Ghosh · P. Srivastava · P. Kumar ·
D. Kanjilal

Received: 25 April 2011 / Accepted: 12 December 2011 / Published online: 8 February 2012
© Springer-Verlag 2012

Abstract We report variable temperature resistivity measurements and mechanisms related to electrical conduction in 200 keV Ni²⁺ ion implanted ZnO thin films deposited by vapor phase transport. The dc electrical resistivity versus temperature curves show that all polycrystalline ZnO films are semiconducting in nature. In the room temperature range they exhibit band conduction and conduction due to thermionic emission of electrons from grain boundaries present in the polycrystalline films. In the low temperature range, nearest neighbor hopping (NNH) and variable range hopping (VRH) conduction are observed. The detailed conduction mechanism of these films and the effects of grain boundary (GB) barriers on the electrical conduction process are discussed. An attempt is made to correlate electrical conduction behavior and previously observed room temperature ferromagnetism of these films.

1 Introduction

Zinc oxide (ZnO), a wide band gap (~3.37 eV) semiconductor, has been extensively studied because of its promising applications in various fields such as electronics, optoelectronics, sensors, spintronics and optospintronics. Most

of these applications demand a detailed understanding of the electrical properties of the material and its variation with temperature. It is known from the literature that non-stoichiometric ZnO is an n-type semiconductor where carrier electrons are excited thermally to the conduction band from the donor levels formed by intrinsic defects such as O-vacancies or Zn interstitials [1, 2]. Along with the native defects, appropriate doping of this material with metallic dopants also modifies electrical behavior of the films and the behavior mainly depends on the doping concentration and crystallinity of the films. The electrical properties of polycrystalline ZnO thin films are found to be different from those of the single crystalline films due to the presence of crystallites (grains) of different sizes and grain boundaries. The grain boundaries present in the film work as a potential barrier for conduction electrons and restrict an electron to move freely in a matrix affecting the conductivity of the film. The presence of grain boundaries also generates interface states in the band structure acting as barriers and traps for the moving electrons in semiconductor materials [3, 4] thereby reducing the overall conductivity of a polycrystalline film. The electrical conduction process at room temperature (RT) and low temperature (LT) has been generally understood by the thermal excitation of electrons from the donor levels generated by defects or impurity atoms to conduction band [5]. In addition to band conduction, the conduction process has also been attributed to the transport involving thermionic and thermal field emission of electrons over grain boundaries in the polycrystalline ZnO films [5–8]. This is because the electrons have sufficient thermal energy to cross the grain boundary barrier at room temperature. However, at temperature lower than room temperature, conduction is believed to be due to nearest neighbor hopping (NNH) and at very low temperature, the conduction process is dominated by variable range hopping (VRH) [5]. All

B. Joshi (✉)
Department of Applied Sciences, Gautam Buddha University,
Greater Noida 201308, India
e-mail: pandeyb44@yahoo.co.in

S. Ghosh · P. Srivastava
Nanotech Laboratory, Indian Institute of Technology Delhi, New
Delhi 110 016, India

P. Kumar · D. Kanjilal
Inter University Accelerator Centre, Aruna Asaf Ali Marg, New
Delhi 110 067 India

these conduction processes also depend on the film synthesis routes, nature of defects, defect levels and the dopants used for any specific purpose. Therefore, it is extremely important to understand the electrical conduction behavior of these films at different temperature ranges before implementing it for any device fabrication.

In our previous works we have demonstrated room temperature ferromagnetism (RT-FM) and transparent ferromagnetism in 200 keV Ni²⁺ ion implanted polycrystalline ZnO films [9, 10] and correlated it with defects and the charge carriers generated due to implantation. This is also influenced by microstructure or crystallinity of the films and hence the grain boundaries can play a crucial role in electron transport, which in turn affects any other physical properties of the film. In this paper we report a detailed study of temperature dependent conductivity of ZnO:Ni films synthesized by implanting 200 keV Ni²⁺ ions on ZnO films [9]. The incident ion fluence values were chosen in such a manner as to obtain quite low metal (maximum up to 7 at%) concentration in ZnO. This paper mainly focuses on different electrical conduction mechanisms present in these films as we go down from room temperature to low temperature. An attempt has also been made here to correlate electrical transport properties with observed ferromagnetism at room temperature.

2 Experimental

Pure ZnO thin films deposited by Vapor Phase Transport (VPT) are implanted with Ni²⁺ ions with fluence values 2×10^{15} , 3×10^{15} and 2×10^{16} ions/cm² to give 2, 3 and

7 at% Ni in the films. Experimental details have already been discussed [9]. Films corresponding to 2, 3 and 7 at% are named A1, A2 and A3, respectively. The dc electrical resistivity of the films is measured by variable temperature resistivity measurement set-up for a temperature range of 20–300 K. For carrying out measurements, a film with four contacts is kept in a chamber which is evacuated by a scroll pump. The chamber is cryogenically cooled up to 20 K for low temperature measurements. Temperature controller (Lake Shore) is used to control and read the temperature of the film. Four contacts made on the film are connected to a source meter (Keithley 2400) for the measurements. The whole system is computer interfaced, where data of resistance versus temperature are recorded for all films.

3 Results and discussion

3.1 Electrical conduction mechanism at around room temperature

The variation of resistivity with temperature for A1–A3 films reveals their semiconducting nature and is shown in Fig. 1. It is to be noted that the resistivity values at room temperature calculated from these data are somewhat higher (having the same order of magnitude) than that reported earlier [9]. This is due to the fact that only one direction of current is considered in this measurement while eight different current directions were taken into consideration (van der Pauw method) previously and hence the measured resistances were averaged out. As mentioned earlier, around

Fig. 1 Resistivity versus temperature of Ni implanted ZnO/Si films (A1, A2, A3). All the curves show the semiconducting nature of the films

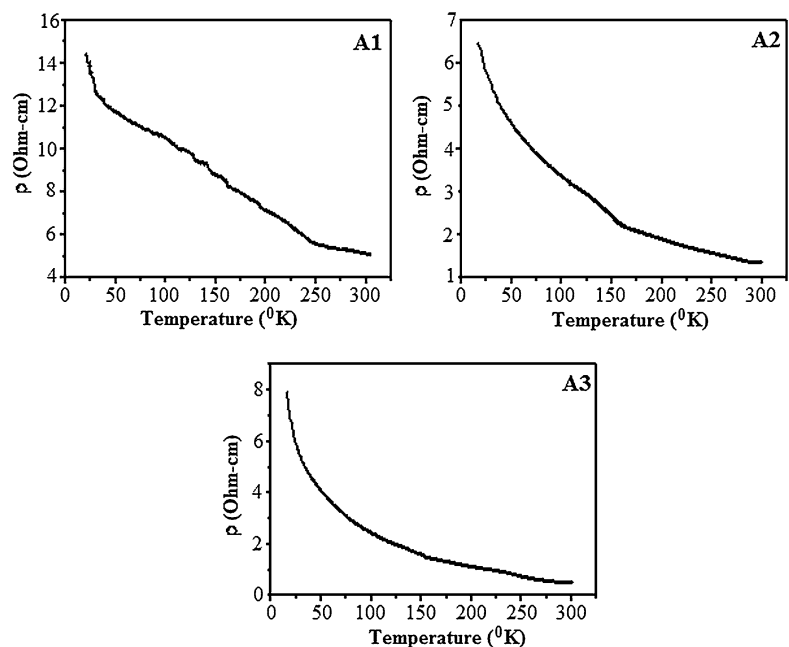
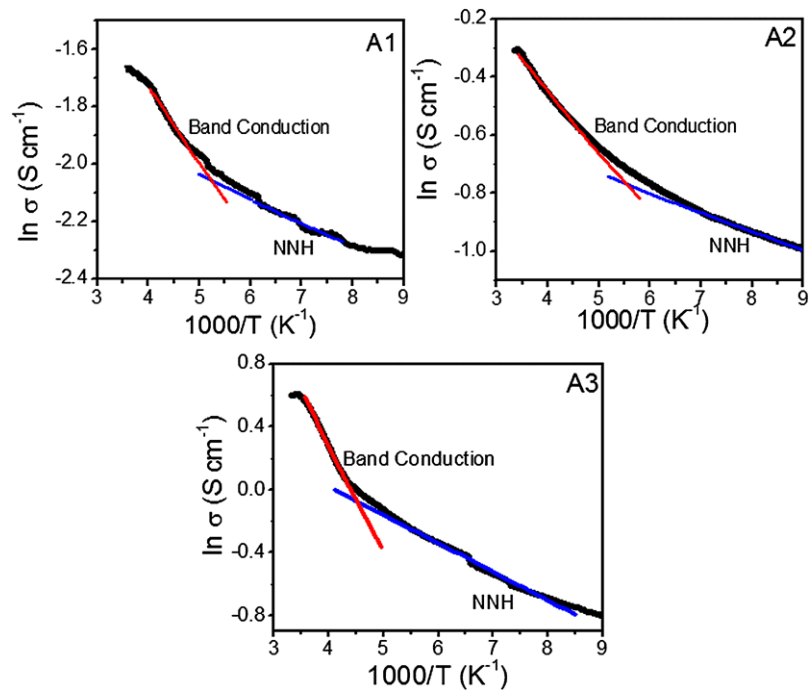


Fig. 2 Arrhenius plot for the Ni implanted ZnO/Si films (A1, A2, A3). Two slopes in the curves show two different conduction mechanisms (band conduction and NNH) in this temperature range



room temperature the main conduction process is band conduction, in which the charge carriers are thermally activated in the conduction band of the film.

According to the literature for thermally activated band conduction, the conductivity (σ) is expressed by [8, 11]

$$\sigma = \sigma_0 \exp\left(-\frac{E_a}{kT}\right) \quad (1)$$

where σ_0 is a pre-exponential factor (i.e. a constant), E_a is the activation energy and k is Boltzmann's constant. Therefore, the activation energy required for this conduction to occur is calculated by plotting a graph between $\ln \sigma$ versus $1000/T$ (Arrhenius plot) and measuring the slope of the curve by linear fitting method (shown in red in Fig. 2) as from (1), $\ln \sigma \propto (-\frac{E_a}{kT})$. Moreover, at temperatures lower than room temperature, most of the free electrons in a doped or non-stoichiometric semiconductor do not have sufficient energy to jump from donor levels to conduction band and are recaptured by donors themselves. However, they conduct by hopping from one impurity level to another, making the thermally activated band conduction less important at lower temperatures. Because of the hopping of electrons from an occupied level to an empty level, the conduction is named hopping conduction [8, 11–17] and both donor and acceptor levels in the impurity band are required for this to occur. Depending upon the temperature range, this conduction mechanism is classified into two different categories viz. Nearest-Neighbor Hopping (NNH) and Variable Range Hopping (VRH) conduction and both are found to play a significant role in the conduction process of ZnO thin films at lower temperature region [5, 8, 11]. These conduction mechanisms are discussed in the next subsection.

Now we would like to point out that in polycrystalline thin films the effect of grain boundaries on the electron transport at around room temperature is of paramount importance and is discussed here based on the work by Orton and Powell [3]. Grain boundaries in a polycrystalline film work as potential barriers for the electrons in the matrix, which in turn influence the overall electrical properties of the film. The effect of grain boundary barriers is examined by evaluation of the Debye screening length (L_D) which is defined as the scale over which mobile charge carriers screen out electric fields in semiconductors. The Debye screening length is mainly compared with the average grain size (l) and is given by the following equation:

$$L_D = \left(\frac{\epsilon \epsilon_0 kT}{e^2 N_d}\right)^{1/2} \quad (2)$$

where ϵ is the specific dielectric constant, ϵ_0 is the dielectric constant of vacuum and N_d is the density of donors in the film. Provided L_D is smaller than $l/2$, a potential barrier around each grain boundary is formed due to band bending. However, if L_D is larger than $l/2$, the conduction band becomes flat and there is no potential barrier. In this particular case electrons are transported without grain boundary scattering [3].

It is clear from the data that for all the implanted films L_D is smaller than $l/2$, where l is the average grain size measured by atomic force micrographs of the films [9] as shown in Fig. 3. On the basis of that we can say that there is potential barrier around each grain boundary of the film and hence grain boundary scattering is effective in all the films influencing overall mobility of electrons in these films,

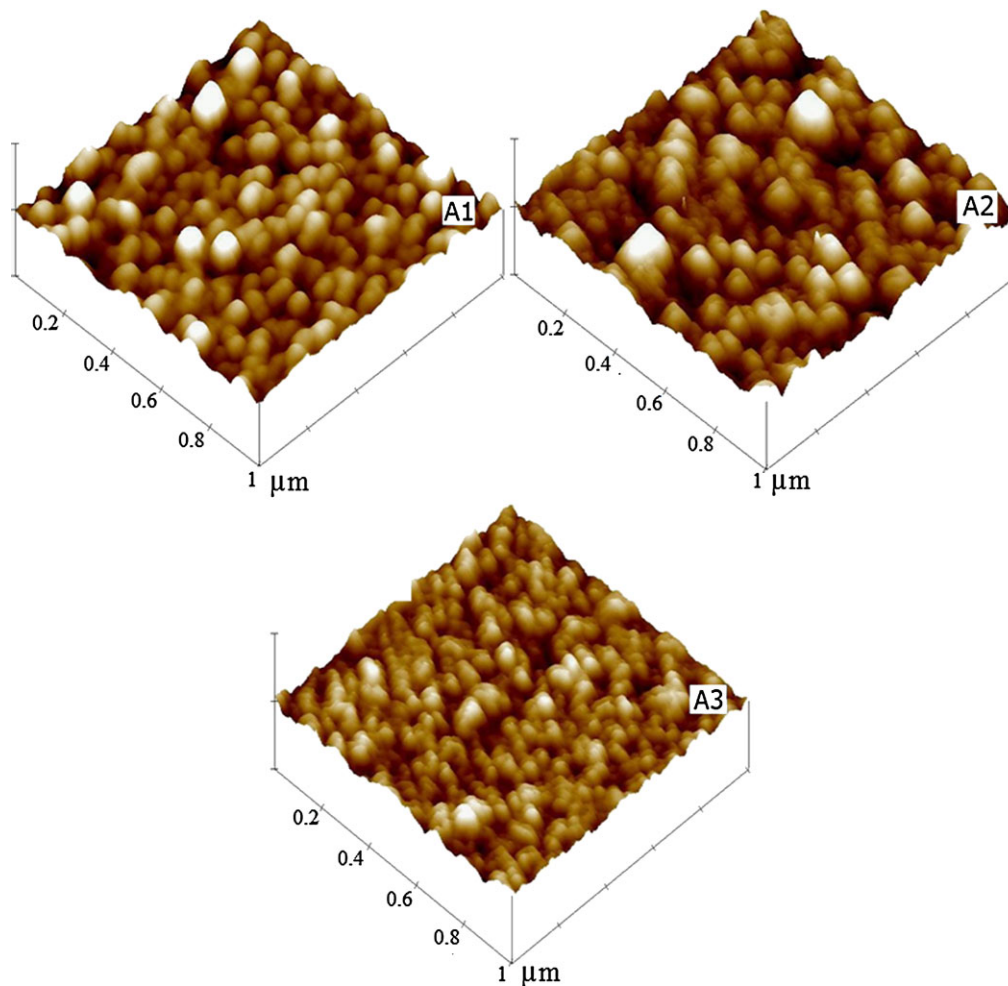


Fig. 3 Atomic force micrographs of films A1–A3, showing the variation in the morphology and grain size of the films with fluence

which in turn affects the other electrical properties of the films.

Now the emissions of charge carriers over the grain boundary barriers present in the polycrystalline films are characterized into two categories, i.e. thermionic emission and thermal field emission as reported by Roth and Williams [6]. And the type of emission present in a particular film can be found by the material tunneling constant, E_{00} which is given as [6]

$$E_{00} = 18.5 \times 10^{-12} \left(\frac{N_d}{m^* \epsilon} \right)^{1/2} \text{ eV} \quad (3)$$

where m^* is the effective mass of electron. According to the literature the mechanism for electrons conducting in the conduction band in polycrystalline semiconductors is analogous to the mechanism for a metal-semiconductor (Schottky) barrier [6, 18, 19]. Therefore, if the semiconductor is at high temperatures or in a low doping range where $kT \gg E_{00}$, the mobility is limited by the thermionic emission of electrons over the grain boundary barriers. On the

other hand, if the semiconductor is at low temperatures or in a high doping range where $kT \ll E_{00}$, the mobility is limited by thermal field emission of electrons through the grain-boundary barriers. If the estimated E_{00} nearly agrees with the value of kT around room temperature, i.e. $kT \sim E_{00}$, then the mobility is limited by both thermionic and thermal-field emission of electrons at the grain-boundary barriers around room temperature.

In these films, E_{00} values (Table 1) calculated from (3) are found to be less than kT (~ 0.026 eV for $T = 300$ K). Hence according to the above discussion, the mobility of electrons in the films is limited by the thermionic emission of electrons over the grain boundary barriers.

As discussed above, if the film is polycrystalline having many grains, the observed conductivity and mobility of the films are affected by the grain boundary barriers present in the films [3]. Now following Seto's work [12], the electrical conductivity due to thermionic emission of charge carriers from grain boundary barriers is given by (4):

Table 1 Various calculated parameters used for explaining the electrical conduction mechanism in the films

Sample	E_{a1} (meV)	E_{a2} (meV)	r (nm)	r/a^*	Av. grain size (nm)	L_D (nm)	E_σ (meV)	E_{00} (eV)
A1	20	6.9	135.1	8.1	80	11.3	32	0.003
A2	18.7	5.6	55.6	3.3	129	2.9	30	0.012
A3	61.7	15.6	52.1	3.1	43	8.5	69	0.004

$$\sigma = \{e^2 N_d / (2\pi m^* kT)^{1/2}\} \times \exp\left\{-\left((E_C - E_F) + e\phi\right)/kT\right\} \quad (4)$$

where E_C is the energy of the conduction band minimum, E_F the Fermi level, ϕ the grain boundary potential barrier and $E_\sigma = E_C - E_F + e\phi$ the activation energy for the grain boundary limited conductivity. From (4) we have $\sigma T^{1/2} \propto \exp(-E_a/kT)$ and it is also evident from Fig. 4 that thermionic emission over grain boundaries exists in these films. The activation energies required to cross the grain boundary potential barrier, E_σ , are listed in the Table 1. The activation energy changes in a similar fashion as band conduction as discussed earlier. This indicates the presence of thermionic emission of electrons from grain boundary barriers in the films and the required activation energy for the emission is least in film A2 and highest in film A3, supporting the other observations in electrical measurements. For all the films, the standard deviation of fits is also calculated which turns out to be almost same and so it is understood that both band conduction and thermionic emission are equally probable in this temperature range.

3.2 Electrical conduction mechanism at low temperature range

At low temperature regime, NNH and VRH are the two major conduction processes, and the difference between NNH and VRH is that the hopping distance traveled by the electrons between the impurity levels is constant in case of NNH, while it varies in VRH conduction. In NNH conduction, an electron hops to the nearest neighbor empty site, which also requires activation energy. However, this activation energy is smaller as compared to that required for thermally activated band conduction [5, 8, 13, 14]. It is generally accepted in the literature that if the variation of $\ln \sigma$ vs. $1000/T$ has two slopes, one at higher (shown by the red line in Fig. 2) and one at lower temperatures (typically below 250 K, shown by the blue line in Fig. 2), this deviation indicates the presence of NNH conduction at a temperature lower than room temperature along with band conduction and therefore double-valued activation energies are observed. Accordingly, (1) is replaced by (5) as given below,

indicating conductivity with the two activation energies for different temperature ranges [8]:

$$\sigma = \sigma_1 \exp\left(-\frac{E_{a1}}{kT}\right) + \sigma_2 \exp\left(-\frac{E_{a2}}{kT}\right) \quad (5)$$

where E_{a1} , E_{a2} are the activation energies required for band and NNH conduction, respectively, σ_1 and σ_2 are the corresponding pre-exponential factors. The values of activation energies in NNH conduction is found to follow the same trend as that of the band conduction and is discussed later.

Now in the VRH conduction mechanism the electrons hop between the levels that are close to the Fermi level irrespective of their spatial distribution. So in this type of hopping conduction the hopping distance is not constant as in NNH conduction [15–17].

According to Hausmann and Teuerle [20], the conduction in In doped ZnO single crystal at temperatures below 300 K is classified into three types when the average spacing between donors r is compared with the effective Bohr radius a^* . Here r and a^* are, respectively, defined as

$$r = \left(\frac{4\pi N_d}{3}\right)^{-1/3}, \quad (6)$$

$$a^* = \frac{0.53\epsilon m}{m^*} \quad (7)$$

where N_d is the impurity (donor) concentration, m is the mass of the free electron, m^* ($\approx 0.3m$) is the effective mass of the electron [21] and ϵ (≈ 8.5) is the specific dielectric constant [22].

The conduction process is classified into three categories depending on the ratios between r and a^* [20]:

1. For $r/a^* > 5$, impurity concentration is low and impurity levels are isolated, and the conduction process is explained by charge transport in the conduction band and the nearest neighbor hopping between isolated donor levels.
2. For $2 < r/a^* < 5$, called the intermediate concentration region, an impurity band is formed by overlap of the wave function between donors. Therefore, variable-range hopping conduction appears between localized states in the impurity band.
3. For $r/a^* < 2$, the high impurity concentration regime, the metallic conduction takes place because of overlapping of impurity and conduction band.

Fig. 4 $\ln(\sigma T^{1/2})$ versus inverse temperature (T^{-1}) Ni implanted ZnO thin films (A1, A2 and A3, respectively) showing the effect of grain boundaries on conduction

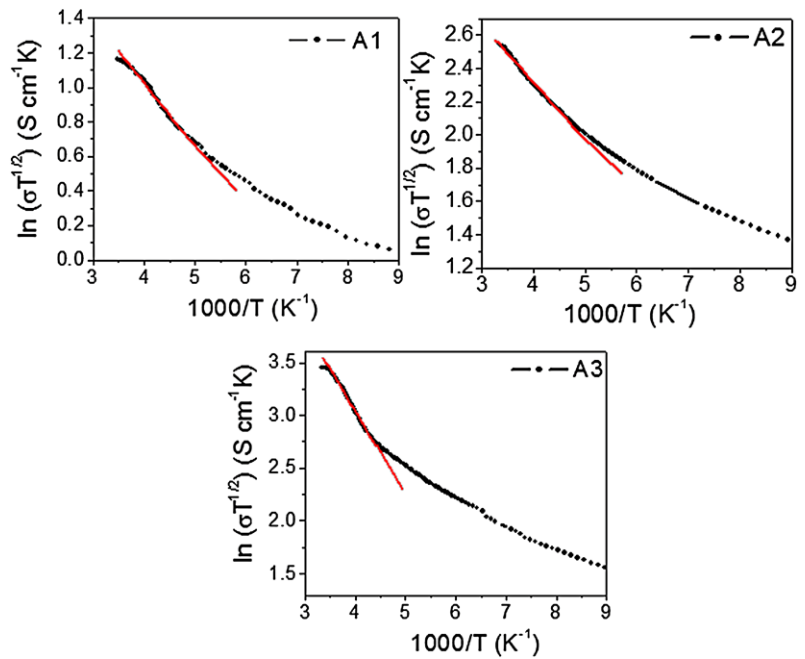
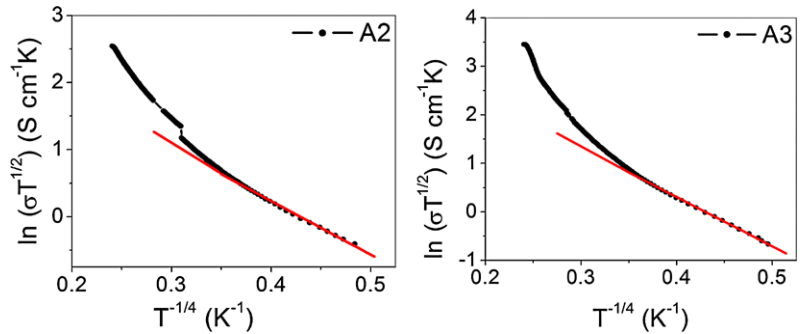


Fig. 5 $\ln(\sigma T^{1/2})$ versus $T^{-1/4}$ for A2, A3 films, showing VRH conduction



We also discuss the mechanism of conduction of the films using these criteria.

The calculated values of r and r/a^* ratio in the films A1, A2 and A3 are shown in Table 1. Here the effective Bohr radius (a^*) calculated from (4) is 16.68 nm.

In case of A2 and A3, the r/a^* ratio from table is 3.3 and 3.1, respectively, which falls in the second category, while in A1, r/a^* is greater than 5 so VRH conduction is absent in film A1. We discuss the VRH mechanism in film A2 and A3.

The relation between conductivity and temperature for VRH conduction is given [23] by

$$\sigma = \sigma_{h0} \exp\left[-\left(\frac{T_0}{T}\right)^{1/4}\right] \tag{8}$$

where σ_{h0} and T_0 are given by the following expressions:

$$\sigma_{h0} = \frac{3e^2 \nu_{ph}}{(8\pi)^{1/2}} \left[\frac{N(E_F)}{\alpha k T} \right]^{1/2}, \tag{9}$$

$$T_0 = \left[\frac{16\alpha^3}{kN(E_F)} \right] \tag{10}$$

where ν_{ph} ($\approx 10^{13} \text{ s}^{-1}$) is the phonon frequency at Debye temperature, k is Boltzmann's constant, $N(E_F)$ is the density of localized electron states at Fermi level and α is the inverse localization length of the localized state.

From (8) and (9)

$$\ln(\sigma T^{1/2}) \propto T^{-1/4} \tag{11}$$

In order to evaluate the possibility of VRH conduction in A2 and A3 films at low temperature, the dc conductivity was plotted according to (11). Figure 5 shows the variation of $\ln(\sigma T^{1/2})$ with $T^{-1/4}$ for the films. The straight line plot at lower temperature range indicates that the dominant mechanism of conduction is VRH in these films.

3.3 Comments on electrical conduction process in the films

Figure 2 shows the Arrhenius plots for A1–A3 films in a temperature range of 300 K to 100 K. Two slopes in the curves show the presence of both types of conduction, i.e. band and NNH conduction as indicated earlier also. Activation energies of all the films are calculated using the slopes

of the curves by means of the best fit technique and it is found that the activation energy first decreases with increase in ion fluence (in A1 to A2 films) while for the maximum fluence (in A3), it again increases significantly (Table 1). In A2, the decrease in the activation energy is in accordance with its smaller resistivity and higher concentration of O-vacancies [9]. Higher activation energy in film A3 can be attributed to the microstructure of this particular film. It has been shown and discussed in our previous work [9] that the average grain size of film A3 gets deteriorated due to a higher fluence of Ni ions and also it is clearly evident from the atomic force micrographs shown in Fig. 3. The reduction in the average grain size generates more interface states, which in turn trap the conduction electrons [9, 24] and do not allow them to get activated easily in the conduction band as compared to A1 and A2. The same holds for the variation of activation energies calculated in case of thermionic emission of electrons from grain boundary barriers present in all the films. A similar trend in activation energy is seen in NNH conduction also. This signifies that although the conduction electrons are present in all three films but due to the different microstructure and presence of dissimilar grain boundaries, the activation of the electrons in the conduction band is significantly different affecting the overall electrical properties of the films. On the basis of mathematical calculations found in the literature, the main conduction process at low temperature, i.e. VRH conduction is found to be present in the films A2 and A3 and not present in film A1 (Fig. 5). This is possibly because of the larger carrier concentration in films A2 and A3 as compared to that in film A1. However, this requires further investigations.

3.4 Correlation between electrical properties and RT-FM

In our earlier work [9] it has been shown that all these films are ferromagnetic at room temperature having highest saturation magnetization in case of film A2 followed by A1 and A3. The defects related to O-vacancies and microstructure of the films are shown to be key factors in their RT-FM properties. Ferromagnetism in these films is considered to be due to exchange interaction mediated by free charge carriers generated by O-vacancies, and hence FM strength scales with this defect [9]. However, in case of film A3 although O-vacancy was observed to be almost the same as that of A2, microstructure plays an influential role to decrease FM strength in A3 [9]. This fact is now analyzed here on the basis of electrical transport behavior of the films discussed in the previous subsection. The increase in FM strength from A1 to A2 can be correlated with the calculated activation energy values. It is observed that from A1 to A2, activation energy in case of both band and NNH conduction decreases, which in turn implies that more charge carriers are activated in conduction band and are delocalized due to which it is

easy for them to take part in the magnetic interaction resulting in an increase in RT-FM strength. However, in film A3 the activation energy increases significantly, making it difficult for the charge carriers to take part in the interaction as they are considered to be more localized. Due to the localization of charge carriers the interaction probability decreases thereby, resulting in a reduction in the RT-FM strength. It is well known that the electrical conduction in thin films is affected by the crystalline structure and morphology of the films, which in turn affect the activation energies. Therefore, the influence of structure and morphology on conduction mechanism as well as ferromagnetic properties lead to a good correlation with each other. Further experimental studies are required to investigate this correlation with more systematic variation in microstructure for films grown by different techniques.

4 Conclusions

Temperature dependent resistivity measurements in 200 keV Ni²⁺ ion implanted ZnO thin films show the semiconducting behavior of these films. Both band and thermionic emission from grain boundary barriers are seen near the room temperature regime. Activation energies calculated by best fitting method marginally decreases with Ni concentration initially (2 at% to 3 at%), and then increases significantly for the maximum Ni (i.e. 7 at%) concentration. This is explained on the basis of deterioration of the microstructure and appearance of more interface states in the film having 7 at% Ni. On the basis of standard deviation calculation, it is found that both band conduction and thermionic emission over the grain boundary are equally probable at around room temperature. However, more experimental investigations are required to determine the contribution of individual processes. In the low temperature range, NNH conduction is found to be present in all the films, however, VRH conduction is present only in 3 and 7 at% Ni implanted ZnO films. Finally, electrical transport properties are correlated with crystallinity and microstructure of the films and an attempt has been made to correlate the result with observed RT-FM properties of these films.

Acknowledgements We are thankful to Dr. Neeraj Khare, IIT Delhi for various important discussions. One of the authors (B. Joshi) gratefully acknowledges the financial support from Department of Science and Technology (DST) and University Grants Commission (UGC), New Delhi.

References

1. F.A. Kröger, *The Chemistry of Imperfect Crystals*, 2nd edn. (North Holland, Amsterdam, 1974)

2. W.D. Kingery, H.K. Bowen, D.R. Uhlmann, *Introduction to Ceramics* (Wiley, New York, 1976), Chap. 4
3. J.W. Orton, M.J. Powell, *Rep. Prog. Phys.* **43**, 1263 (1980)
4. L.L. Kazmerski, *Polycrystalline and Amorphous Thin Films & Devices* (Academic Press, New York, 1980)
5. Y. Natsume, H. Sakata, T. Hirayama, H. Yanagida, *J. Appl. Phys.* **72**, 4202 (1992)
6. A.P. Roth, D.F. Williams, *J. Appl. Phys.* **52**, 6686 (1981)
7. R.L. Petritz, *Phys. Rev.* **104**, 1508 (1956)
8. Y. Natsume, H. Sakata, *Thin Solid Films* **372**, 30 (2000)
9. B. Pandey, S. Ghosh, P. Srivastava, P. Kumar, D. Kanjilal, *J. Appl. Phys.* **105**, 033909 (2009)
10. B. Pandey, S. Ghosh, P. Srivastava, D. Kanjilal, P. Kumar, S. Zhou, H. Schmidt, *J. Appl. Phys.* **107**, 023901 (2010)
11. R. Kumar, N. Khare, *Thin Solid Films* **516**, 1302 (2008)
12. J.Y.W. Seto, *J. Appl. Phys.* **46**, 5247 (1975)
13. J. Han, M. Shen, W. Cao, A.M.R. Senos, P.Q. Mantas, *Appl. Phys. Lett.* **82**, 67 (2003)
14. A. Miller, E. Abrahams, *Phys. Rev.* **120**, 745 (1960)
15. S. Bandyopadhyay, G.K. Paul, R. Roy, S.K. Sen, S. Sen, *Mater. Chem. Phys.* **74**, 83 (2002)
16. Y.Z. Yoo, T. Fukumura, Z. Jin, K. Hasegawa, M. Kawasaki, P. Ahmet, T. Chikyow, H. Koinuma, *J. Appl. Phys.* **90**, 4246 (2001)
17. O.D. Jayakumar, I.K. Gopalakrishnan, S.K. Kulshreshtha, *J. Mater. Chem.* **15**, 3514 (2005)
18. F.A. Padovani, R. Stratton, *Solid-State Electron.* **9**, 695 (1966)
19. C.R. Crowell, V.L. Rideout, *Solid-State Electron.* **12**, 89 (1969)
20. A. Hausmann, W. Teuerle, *Z. Phys.* **257**, 299 (1972)
21. D.C. Reynolds, C.W. Litton, T.C. Collins, *Phys. Status Solidi* **12**, 3 (1965)
22. A.R. Hutson, *J. Appl. Phys.* **32**, 2287 (1961)
23. N.F. Mott, *J. Non-Cryst. Solids* **1**, 1 (1968)
24. W. Yu, L.H. Yang, X.Y. Teng, J.C. Zhang, L. Zhang, G.S. Fu, *J. Appl. Phys.* **103**, 093901 (2008)